# Enhancement in thermoelectric performance of n-type Pb-deficit Pb-Sb-Te alloys

Bhuvanesh Srinivasan, Francesco Gucci, Catherine Boussard-Plédel, François Cheviré, Michael J. Reece, Sylvain Tricot, Laurent Calvez, Bruno Bureau

# Enhancement in Thermoelectric Performance of n-type Pb-deficit Pb-Sb-Te Alloys

Bhuvanesh Srinivasan*[a], Francesco Gucci[b], Catherine Boussard-Pledel[a], François Cheviré[a], Michael J. Reece[b], Sylvain Tricot[c], Laurent Calvez[a] and Bruno Bureau*[a]

[a] Équipe Verres et Céramiques (V&C), ISCR CNRS UMR 6226, Université de Rennes 1, Rennes 35042, France

[b] School of Engineering and Materials Science, Queen Mary University of London, London E1 4NS, United Kingdom

[c] Institut de Physique de Rennes, CNRS UMR 6251-Université de Rennes 1, Rennes 35042, France

* Correspondence: bhuvanesh.srinivasan@univ-rennes1.fr; Tel.: +33-223233688

bruno.bureau@univ-rennes1.fr; Tel.: +33-223236573; Fax: +33-223235611

† *Electronic Supplementary Information (ESI) available*



**Abstract**

PbTe based materials are well known for their high performance thermoelectric properties. Here, a systematic study of thermoelectric transport properties of n-type Pb-deficit $Pb_{0.98-x}Sb_xTe$ alloys with carrier concentrations in the range of ~$10^{-19}$ $cm^{-3}$ is presented from room temperature to 623 K. A maximum thermoelectric figure of merit (zT) of ~0.81 was achieved at 623 K for 4 mol% Sb containing Pb-deficit composition, by the cumulative integration of enhanced power factor and significant reduction in thermal conductivity. The scattering of phonons at Pb vacancies, contributed to the reduction of lattice thermal conductivity, and thereby strikingly boosted the zT of the Pb-deficit samples when compared with the pristine $Pb_{1-x}Sb_xTe$.

**Keywords**: Thermoelectrics; Pb-deficit lead tellurides; Sb alloying; Low thermal conductivity; Improved figure of merit.

**Graphical Abstract**

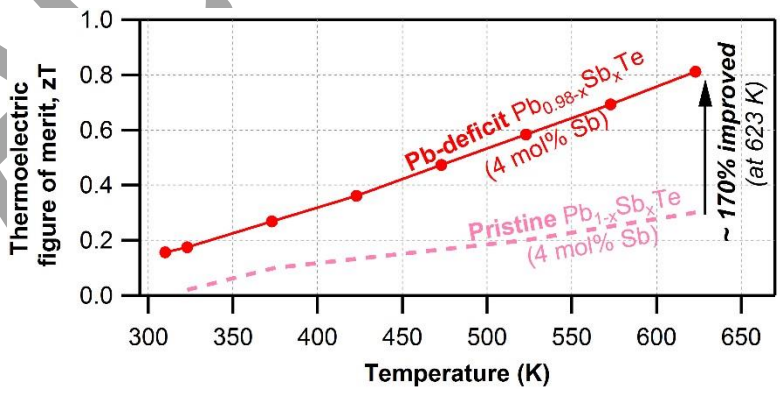


## 1. Introduction

For several decades, thermoelectric materials (TE) and devices have drawn increasing interest and attention due to their potential to convert waste heat into useful electricity. The efficiency of a TE material

is quantified by a dimensionless figure of merit, $zT = S^2\sigma T/\kappa$ where S, σ, T and κ are Seebeck coefficient, electrical conductivity, temperature and total thermal conductivity (sum of the electronic part, $\kappa_e$ and the lattice part, $\kappa_{latt}$) respectively. The fact that these transport properties are highly interrelated, presents a great challenge in attempting to enhancing zT. Advances in recent times show that it is feasible to enhance zT by a number of approaches [1–4]. One approach is solid solution alloying, which enables acoustic phonon scattering leading to a decreased $\kappa_{latt}$ [5–10].

Among several kinds of TE materials, PbTe has demonstrated a relatively high zT value ($zT \sim 1$) at mid-temperature ranges and is one of the most studied material [11] with an array of alloying materials and strategies to optimize its carrier concentration [12,13], manipulate its band structure [14–19] and to achieve nanostructuring [6,20–26]. Our investigation of the thermoelectric properties of $Pb_{0.98-x}Sb_xTe$ system was motivated by a past study on the n-type self-deficit $Pb_{0.96}Sb_{0.02}Te_{1-x}Se_x$ bulk materials, where a strong reduction of $\kappa_{latt}$ and an enhanced zT was reported [27]. Improvising on that work, where the Sb content was kept fixed while the Se content was varied, herein we try to understand the effect of variation of Sb content on the thermoelectric properties of Se-free $Pb_{0.98-x}Sb_xTe$ solid solutions and to compare the performance of these Pb-deficit samples with that of previously reported [28] pristine $Pb_{1-x}Sb_xTe$ compositions. Though several works have been done in the past to exploit the thermoelectric phenomenon in PbTe based alloys, including Sb doped PbTe, not much information is available on the Sb doped, Pb deficient composition ($Pb_{0.98}Te$). The choice of Sb was also motivated by the ab-initio calculations of the effect of Sb impurities on the electronic structure of PbTe, which pointed to the presence of resonance states at the bottom of the conduction band and a possible enhancement of the Seebeck coefficient for optimal Sb concentration [17].

Herein, we report a significant improvement in the thermoelectric performance of Pb-deficit $Pb_{0.98-x}Sb_xTe$ samples, when compared to its pristine $Pb_{1-x}Sb_xTe$ composition.

## 2. Materials and Methods

The samples of $Pb_{0.98-x}Sb_xTe$ ($x = 0.01 – 0.12$) were synthesized by vacuum sealed-tube melting processing. The ampoules with appropriate stoichiometric amounts of high purity starting elements (Pb, Sb and Te) were sealed under a vacuum of $10^{-6}$ Torr, then placed in a rocking furnace and slowly heated up to 1223 K over a period of 12 hours, then held at that temperature for 12 hours and slowly cooled down to room temperature over 24 hours. The obtained ingots were cut and polished to required shapes and dimensions for various thermoelectric measurements. Powder X-ray diffraction (PXRD) patterns were recorded at room temperature in the 2θ range 5-120° with step size of 0.026° and a scan per step of 400s using a PANalytical X'Pert Pro diffractometer (Cu K-$L_{2,3}$ radiation, PIXcel 1D detector). The Hall measurements were carried on samples of dimensions ~5x5x2 $mm^3$ using a four-point probe setup (Van der Pauw method), where a fixed magnetic field of 0.112 T and DC current of 15 mA was applied. The electrical conductivity and Seebeck coefficients were measured simultaneously from room temperature to 623 K on samples of dimension ~10x2x2 $mm^3$ using a commercial instrument (LSR-3, Linseis Inc.), in a He atmosphere. Temperature dependent thermal diffusivity, D, was measured on disc shaped samples of dimension ~10 mm diameter x 2 mm thickness using the laser flash diffusivity method in a Netzsch LFA-457. The heat capacity, $C_p$, was derived using the Dulong–Petit relation, $C_p = 3R/M$ (R is the gas constant and M is the molar mass). The total thermal conductivity was obtained from the equation, $\kappa = DC_p\rho$, where

ρ is the density of the sample measured using Archimedes' principle. The uncertainty in the results for the values of Hall measurement, electrical and thermal transport properties are ~2%, ~5% and ~7% respectively and that for zT value is 12%. Error bars are not shown in the figures to increase the readability of the curves. Refer supporting information (*ESI†*) for microscopic analysis and details regarding the estimation of electronic and lattice contributions to thermal conductivity.

### 3. Results and discussion

Powder XRD patterns of all of the samples are presented in figure 1 (a). Sharp peaks indicate the polycrystalline nature of the phases. The main peaks could be indexed to a cubic PbTe phase. $Sb_2Te_3$ secondary phase is observed at higher concentrations of the dopant (≥ 4 mol% Sb), indicating a low solubility limit for Sb in PbTe. Still the decrease of lattice parameter with Sb content, as shown in figure 1 (b), suggests some substitution of smaller $Sb^{3+}$ atoms (~1.45 Å) for larger $Pb^{2+}$ atoms (~1.8 Å). The non-linear evolution of the lattice parameter at higher Sb contents indicates that Sb is not fully substituted for Pb in the whole composition range, confirming its low solubility in PbTe. SEM-EDX analysis are in agreement with the XRD results (see *ESI†*).

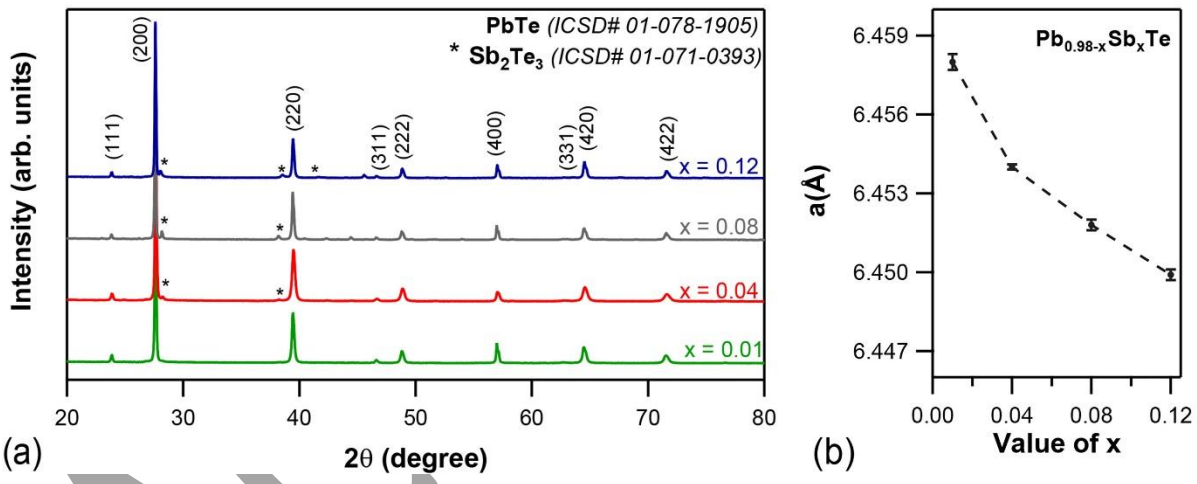


***Figure 1.*** *(a) PXRD patterns for $Pb_{0.98-x}Sb_xTe$ samples, (b) Lattice parameter as a function of Sb content.*

***Table 1.*** *Hall measurement results (at 300 K) of carrier concentration, n and mobility, μ for $Pb_{0.98-x}Sb_xTe$ samples*

| **Sample** Notation | ***$Pb_{0.98-x}Sb_xTe$*** Value of x | **n** ($10^{19}$ $cm^{-3}$) | **μ** ($cm^2V^{-1}s^{-1}$) |
|---|---|---|---|
| PST-1 | 0.01 | 0.38 | 330.9 |
| PST-4 | 0.04 | 1.99 | 677.45 |
| PST-8 | 0.08 | 1.36 | 518.84 |
| PST-12 | 0.12 | 3.65 | 317.34 |

The results from Hall measurements tabulating carrier concentration (n) and mobility (μ) are presented in Table 1. As the Hall voltage is negative in all these samples, electrons are the major charge carriers (n-type). The electrical transport properties of the different compositions are presented in figure

2 (a) and (b). The negative Seebeck coefficients confirms the n-type charge carriers in the samples. The linear increase of the absolute Seebeck coefficient and the monotonic decrease in electrical conductivity with increasing temperature suggests degenerate semiconducting behavior for most of the samples [29–31]. These tendencies, expected due to a slight loss of degeneracy at elevated temperatures [13], allow the assumption of single band conduction behavior for these samples within the values of carrier density and temperature ranges studied. The carrier density does not follow any specific trend, and such anomalous changes, which are difficult to explain have been reported for other such self-compensated compositions [32,33]. It must also be noted that the carrier densities for these Pb-deficit $Pb_{0.98-x}Sb_xTe$ compositions are almost one order of magnitude higher than undoped PbTe ($n \sim 1.11 \times 10^{-18}$ $cm^{-1}$) [13], due to the aliovalent donor doping of $Sb^{3+}$ in the $Pb^{2+}$ sub-lattices of PbTe. Interestingly, Sb is known to be an amphoteric dopant depending on its lattice position [34], which means that in Te-rich PbTe, Sb substitutes for Pb (donor) and in Pb-rich PbTe, Sb substitutes for Te (acceptor). Despite PST-12 having twice the n-values of PST-8, its carrier charge mobility is reduced by half and this cumulative effect is observed in fig. 2(a), where the σ of both these samples are almost the same. The S-value for these samples at room temperature are in the range of -50 to -200 μV/K, while at 623 K it reaches a maximum of -300 μV/K for PST-1 and -193 μV/K for PST-4. The Seebeck results are coherent (inverse proportionality) with the carrier densities obtained by Hall measurements. The thermoelectric power factor, $P.F = S^2\sigma$, as shown in fig 2(c) reaches more than $1.7 \times 10^{-3}$ $W/mK^2$ at mid-temperature ranges for PST-4, which is on par with other PbTe based materials [12]. The power factor does not vary much beyond 500 K for PST-4 and PST-12, whereas the power factor slumps continuously for PST-1 and PST-8, just like in LAST alloys [15]. The reduction in mobility with increasing Sb content can be attributed to the dopant scattering, arising due to solid solution alloying. PST-4 has an increased carrier mobility, possibly arising from its interesting microstructure (with lamellar growth domains and different grain sizes), as shown in *ESI†*. The transport properties of the constituent phases (PbTe and $Sb_2Te_3$) are tabulated in *ESI†*.

The total thermal conductivity of the PST samples and its lattice contributions are presented in figure 2(d). At room temperature, the κ value for the samples varies from 1.9 to 2.9 W/mK and the values drops to lower than 1.5 at 623 K. The lowest value of κ is exhibited by PST-1 (1.1 W/mK), followed by PST-4 (1.25 W/mK), which are lower than other well-known n-type PbTe based high performance materials (κ < 1.5 w/mK) with the similar carrier concentration values [13]. This can be due to the increased disorder created by Sb doping in the self-deficit PbTe lattice, leading to a decreased lattice contribution. Moreover, as reported by Zhu et al [35]., there is also an increase of anharmonic coupling between heat carrying phonons, causing their mutual scattering with increasing temperature. For PST-4 and PST-12, an ultra-low $\kappa_{latt}$ of ~0.8 W/mK was achieved at 623 K, competing well with state of the art TE materials (κ < 1 W/mK). The aliovalent donor substitution of $Sb^{3+}$ for $Pb^{2+}$ is not balanced by the acceptor action of the vacancies formed in the PbTe sub-lattice [36], thus resulting in the lower thermal conductivity.

A plot of the temperature dependent thermoelectric figure of merit, zT is presented in figure 2(e). In Pb-deficit compositions, the highest zT of ~0.81 is achieved at 623 K for the 4 mol% Sb containing sample. Both of the 1 mol% and 12 mol% Sb containing samples exhibit zT of ~0.6 at 623 K. The zT values of these self-deficit $Pb_{0.98-x}Sb_xTe$ compositions are much higher than the values for pristine $Pb_{1-x}Sb_xTe$ compositions reported by Dow et al., [28]. For instance, the 4 mol% Sb containing Pb-deficit sample with the nominal composition $Pb_{0.94}Sb_{0.04}Te$ exhibits zT of ~0.81 at 623 K. While it was reported that, for the same dopant concentration in pristine composition ($Pb_{0.96}Sb_{0.04}Te$), the zT obtained was only ~0.3 at the

same temperature [28]. In the case of pristine compositions, the highest value of zT obtained at 623 K was only ~0.5 for $Pb_{0.9}Sb_{0.1}Te$, which then reaches to a maximum of ~0.6 at 723 K.

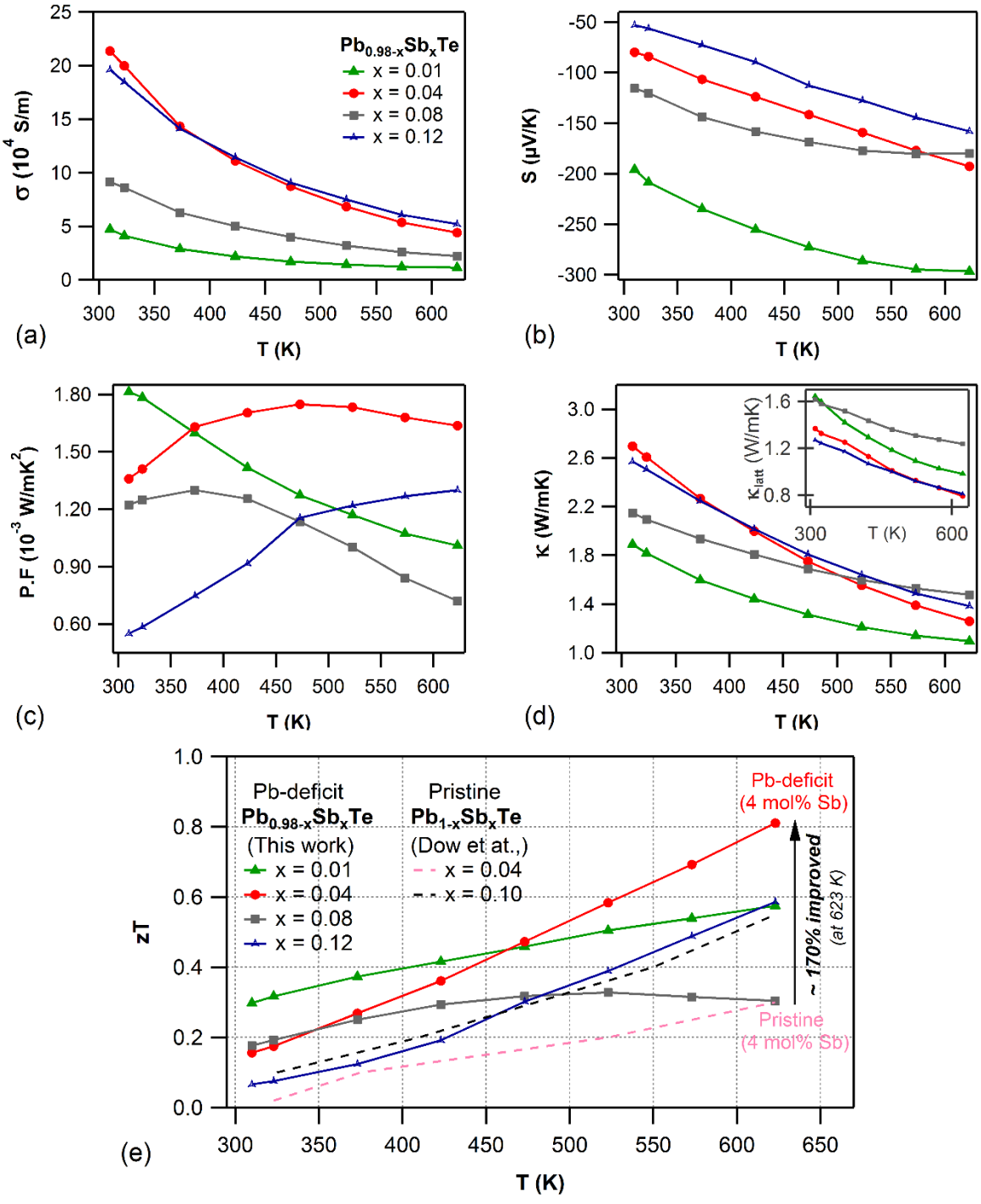


***Figure 2****. Temperature dependent transport properties – (a) Electrical conductivity, σ (b) Seebeck coefficient, S (c) Power Factor, P.F (d) Total thermal conductivity, κ and Lattice thermal conductivity, $\kappa_{latt}$ in the insert (e) Figure of merit, zT.*

The better TE performance of Pb-deficit samples is due to their better electrical conductivity and lower thermal conductivity when compared to pristine $Pb_{1-x}Sb_xTe$ [28]. This reduction in $\kappa$ for self-deficient samples is expected to arise from phonon-scattering at the vacancies, which act as point-defects [37] and suppresses the lattice contribution by about 50%, when compared with pristine $Pb_{1-x}Sb_xTe$ [28]. A high temperature extrapolation of the linear temperature dependence zT plot of Pb-deficit composition containing 4 mol% Sb indicates a possible figure of merit of ~1.3 at 850 K, making them a serious candidate for high temperature TE applications.

## 4. Conclusion

To summarize, high quality crystalline ingots of $Pb_{0.98-x}Sb_xTe$ were obtained by vacuum sealed-tube melting processing. Reduction in the lattice parameter confirmed the aliovalent donor substitution of $Sb^{3+}$ for $Pb^{2+}$ in PbTe, but the solubility limit was found to be minimum. These Sb-doped, Pb-deficit, n-type samples exhibited high carrier densities (~$10^{-19}$ $cm^{-3}$). Sb alloying reduces the mobility of charge carriers due to dopant scattering and the thermal conductivities were significantly reduced due to the phonon scattering at the vacancies of these Pb-deficit samples. The combination of ultra-low $\kappa_{latt}$ of ~0.8 W/mK and power factors in excess of 1.5 x $10^{-3}$ $W/mK^2$ at around 600 K, for 4 mol% Sb alloying, markedly enhanced the zT from ~0.3 in pristine samples to ~0.81 in Pb-deficit samples.


## Acknowledgment

The research leading to these results has received funding from European Commission's Horizon 2020 research and innovation program under the Marie Sklodowska-Curie ITN actions (GA. 642557; CoACH).


## References


[1] J.R. Sootsman, D.Y. Chung, M.G. Kanatzidis, New and Old Concepts in Thermoelectric Materials, Angew. Chem. Int. Ed. 48 (2009) 8616–8639. doi:10.1002/anie.200900598.

[2] P. Vaqueiro, A.V. Powell, Recent developments in nanostructured materials for high-performance thermoelectrics, J. Mater. Chem. 20 (2010) 9577–9584. doi:10.1039/C0JM01193B.

[3] M.S. Dresselhaus, G. Chen, M.Y. Tang, R.G. Yang, H. Lee, D.Z. Wang, Z.F. Ren, J.-P. Fleurial, P. Gogna, New Directions for Low-Dimensional Thermoelectric Materials, Adv. Mater. 19 (2007) 1043–1053. doi:10.1002/adma.200600527.

[4] Z.-G. Chen, G. Han, L. Yang, L. Cheng, J. Zou, Nanostructured thermoelectric materials: Current research and future challenge, Prog. Nat. Sci. Mater. Int. 22 (2012) 535–549. doi:10.1016/j.pnsc.2012.11.011.

[5] H. Wang, A.D. LaLonde, Y. Pei, G.J. Snyder, The Criteria for Beneficial Disorder in Thermoelectric Solid Solutions, Adv. Funct. Mater. 23 (2013) 1586–1596. doi:10.1002/adfm.201201576.

[6] S.-H. Lo, J. He, K. Biswas, M.G. Kanatzidis, V.P. Dravid, Phonon Scattering and Thermal Conductivity in p-Type Nanostructured PbTe-BaTe Bulk Thermoelectric Materials, Adv. Funct. Mater. 22 (2012) 5175–5184. doi:10.1002/adfm.201201221.

[7] M. Ohta, K. Biswas, S.-H. Lo, J. He, D.Y. Chung, V.P. Dravid, M.G. Kanatzidis, Enhancement of Thermoelectric Figure of Merit by the Insertion of MgTe Nanostructures in p-type PbTe Doped with $Na_2Te$, Adv. Energy Mater. 2 (2012) 1117–1123. doi:10.1002/aenm.201100756.
[8] A. Bali, R. Chetty, A. Sharma, G. Rogl, P. Heinich, S. Suwas, D.K. Misra, P. Rogl, E. Bauer, R.C. Mallik, Thermoelectric properties of In and I doped PbTe, J. Appl. Phys. 120 (2016) 175101. doi:10.1063/1.4965865.
[9] M. Samanta, K. Biswas, Low Thermal Conductivity and High Thermoelectric Performance in $(GeTe)_{1-2x}(GeSe)_x(GeS)_x$: Competition between Solid Solution and Phase Separation, J. Am. Chem. Soc. 139 (2017) 9382–9391. doi:10.1021/jacs.7b05143.
[10] M.K. Jana, K. Pal, A. Warankar, P. Mandal, U.V. Waghmare, K. Biswas, Intrinsic Rattler-Induced Low Thermal Conductivity in Zintl Type $TlInTe_2$, J. Am. Chem. Soc. 139 (2017) 4350–4353. doi:10.1021/jacs.7b01434.
[11] A.D. LaLonde, Y. Pei, H. Wang, G. Jeffrey Snyder, Lead telluride alloy thermoelectrics, Mater. Today. 14 (2011) 526–532. doi:10.1016/S1369-7021(11)70278-4.
[12] Y. Pei, Z.M. Gibbs, A. Gloskovskii, B. Balke, W.G. Zeier, G.J. Snyder, Optimum Carrier Concentration in n-Type PbTe Thermoelectrics, Adv. Energy Mater. 4 (2014) 1400486. doi:10.1002/aenm.201400486.
[13] A.D. LaLonde, Y. Pei, G.J. Snyder, Reevaluation of $PbTe_{1-x}I_x$ as high performance n-type thermoelectric material, Energy Environ. Sci. 4 (2011) 2090–2096. doi:10.1039/C1EE01314A.
[14] J.P. Heremans, V. Jovovic, E.S. Toberer, A. Saramat, K. Kurosaki, A. Charoenphakdee, S. Yamanaka, G.J. Snyder, Enhancement of Thermoelectric Efficiency in PbTe by Distortion of the Electronic Density of States, Science. 321 (2008) 554–557. doi:10.1126/science.1159725.
[15] M.-K. Han, K. Hoang, H. Kong, R. Pcionek, C. Uher, K.M. Paraskevopoulos, S.D. Mahanti, M.G. Kanatzidis, Substitution of Bi for Sb and its Role in the Thermoelectric Properties and Nanostructuring in $Ag_{1-x}Pb_{18}MTe_{20}$ (M = Bi, Sb) (x = 0, 0.14, 0.3), Chem. Mater. 20 (2008) 3512–3520. doi:10.1021/cm703661g.
[16] Y. Pei, X. Shi, A. LaLonde, H. Wang, L. Chen, G.J. Snyder, Convergence of electronic bands for high performance bulk thermoelectrics, Nature. 473 (2011) 66–69. doi:10.1038/nature09996.
[17] D. Bilc, S.D. Mahanti, E. Quarez, K.-F. Hsu, R. Pcionek, M.G. Kanatzidis, Resonant States in the Electronic Structure of the High Performance Thermoelectrics $AgPb_mSbTe_{2+m}$: The Role of Ag-Sb Microstructures, Phys. Rev. Lett. 93 (2004) 146403. doi:10.1103/PhysRevLett.93.146403.
[18] Q. Zhang, F. Cao, W. Liu, K. Lukas, B. Yu, S. Chen, C. Opeil, D. Broido, G. Chen, Z. Ren, Heavy Doping and Band Engineering by Potassium to Improve the Thermoelectric Figure of Merit in p-Type PbTe, PbSe, and $PbTe_{1-y}Se_y$, J. Am. Chem. Soc. 134 (2012) 10031–10038. doi:10.1021/ja301245b.
[19] S. Roychowdhury, U.S. Shenoy, U.V. Waghmare, K. Biswas, Tailoring of Electronic Structure and Thermoelectric Properties of a Topological Crystalline Insulator by Chemical Doping, Angew. Chem. Int. Ed. 54 (2015) 15241–15245. doi:10.1002/anie.201508492.
[20] L.D. Zhao, H.J. Wu, S.Q. Hao, C.I. Wu, X.Y. Zhou, K. Biswas, J.Q. He, T.P. Hogan, C. Uher, C. Wolverton, V.P. Dravid, M.G. Kanatzidis, All-scale hierarchical thermoelectrics: MgTe in PbTe facilitates valence band convergence and suppresses bipolar thermal transport for high performance, Energy Environ. Sci. 6 (2013) 3346–3355. doi:10.1039/C3EE42187B.
[21] P. Jood, M. Ohta, M. Kunii, X. Hu, H. Nishiate, A. Yamamoto, M.G. Kanatzidis, Enhanced average thermoelectric figure of merit of n-type $PbTe_{1-x}I_x$–MgTe, J. Mater. Chem. C. 3 (2015) 10401–10408. doi:10.1039/C5TC01652E.
[22] G. Tan, F. Shi, S. Hao, L.-D. Zhao, H. Chi, X. Zhang, C. Uher, C. Wolverton, V.P. Dravid, M.G. Kanatzidis, Non-equilibrium processing leads to record high thermoelectric figure of merit in PbTe–SrTe, Nat. Commun. 7 (2016) 12167. doi:10.1038/ncomms12167.

[23] K. Ahn, K. Biswas, J. He, I. Chung, V. Dravid, M.G. Kanatzidis, Enhanced thermoelectric properties of p-type nanostructured PbTe–MTe (M = Cd, Hg) materials, Energy Environ. Sci. 6 (2013) 1529–1537. doi:10.1039/C3EE40482J.

[24] Z.-Y. Li, J.-F. Li, Fine-Grained and Nanostructured $AgPb_mSbTe_{m+2}$ Alloys with High Thermoelectric Figure of Merit at Medium Temperature, Adv. Energy Mater. 4 (2014) 300937. doi:10.1002/aenm.201300937.

[25] P.F.P. Poudeu, J. D'Angelo, A.D. Downey, J.L. Short, T.P. Hogan, M.G. Kanatzidis, High Thermoelectric Figure of Merit and Nanostructuring in Bulk p-type $Na_{1-x}Pb_mSb_yTe_{m+2}$, Angew. Chem. Int. Ed. 45 (2006) 3835–3839. doi:10.1002/anie.200600865.

[26] J.R. Sootsman, H. Kong, C. Uher, J.J. D'Angelo, C.-I. Wu, T.P. Hogan, T. Caillat, M.G. Kanatzidis, Large Enhancements in the Thermoelectric Power Factor of Bulk PbTe at High Temperature by Synergistic Nanostructuring, Angew. Chem. Int. Ed. 47 (2008) 8618–8622. doi:10.1002/anie.200803934.

[27] P.F.P. Poudeu, J. D'Angelo, H. Kong, A. Downey, J.L. Short, R. Pcionek, T.P. Hogan, C. Uher, M.G. Kanatzidis, Nanostructures versus Solid Solutions: Low Lattice Thermal Conductivity and Enhanced Thermoelectric Figure of Merit in $Pb_{9.6}Sb_{0.2}Te_{10-x}Se_x$ Bulk Materials, J. Am. Chem. Soc. 128 (2006) 14347–14355. doi:10.1021/ja0647811.

[28] H.S. Dow, M.W. Oh, B.S. Kim, S.D. Park, B.K. Min, H.W. Lee, D.M. Wee, Effect of Ag or Sb addition on the thermoelectric properties of PbTe, J. Appl. Phys. 108 (2010) 113709. doi:10.1063/1.3517088.

[29] B. Srinivasan, C. Boussard-Pledel, V. Dorcet, M. Samanta, K. Biswas, R. Lefèvre, F. Gascoin, F. Cheviré, S. Tricot, M. Reece, B. Bureau, Thermoelectric Properties of Highly-Crystallized Ge-Te-Se Glasses Doped with Cu/Bi, Materials. 10 (2017) 328. doi:10.3390/ma10040328.

[30] S. Perumal, S. Roychowdhury, D.S. Negi, R. Datta, K. Biswas, High Thermoelectric Performance and Enhanced Mechanical Stability of p-type $Ge_{1-x}Sb_xTe$, Chem. Mater. 27 (2015) 7171–7178. doi:10.1021/acs.chemmater.5b03434.

[31] B. Srinivasan, S. Cui, C. Prestipino, A. Gellé, C. Boussard-Pledel, S. Ababou-Girard, A. Trapananti, B. Bureau, S. Di Matteo, Possible Mechanism for Hole Conductivity in Cu–As–Te Thermoelectric Glasses: A XANES and EXAFS Study, J. Phys. Chem. C. 121 (2017) 14045–14050. doi:10.1021/acs.jpcc.7b04555.

[32] A. Banik, U.S. Shenoy, S. Anand, U.V. Waghmare, K. Biswas, Mg Alloying in SnTe Facilitates Valence Band Convergence and Optimizes Thermoelectric Properties, Chem. Mater. 27 (2015) 581–587. doi:10.1021/cm504112m.

[33] R. Al Rahal Al Orabi, N.A. Mecholsky, J. Hwang, W. Kim, J.-S. Rhyee, D. Wee, M. Fornari, Band Degeneracy, Low Thermal Conductivity, and High Thermoelectric Figure of Merit in SnTe–CaTe Alloys, Chem. Mater. 28 (2016) 376–384. doi:10.1021/acs.chemmater.5b04365.

[34] C.M. Jaworski, J. Tobola, E.M. Levin, K. Schmidt-Rohr, J.P. Heremans, Antimony as an amphoteric dopant in lead telluride, Phys. Rev. B. 80 (2009) 125208. doi:10.1103/PhysRevB.80.125208.

[35] P. Zhu, Y. Imai, Y. Isoda, Y. Shinohara, X. Jia, G. Zou, Carrier-Concentration-Dependent Transport and Thermoelectric Properties of PbTe Doped with $Sb_2Te_3$, Mater. Trans. 46 (2005) 2690–2693. doi:10.2320/matertrans.46.2690.

[36] P. Zhu, Y. Imai, Y. Isoda, Y. Shinohara, X. Jia, G. Zou, Enhanced thermoelectric properties of PbTe alloyed with $Sb_2Te_3$, J. Phys. Condens. Matter. 17 (2005) 7319. doi:10.1088/0953-8984/17/46/015.

[37] M.K. Jana, K. Pal, U.V. Waghmare, K. Biswas, The Origin of Ultralow Thermal Conductivity in InTe: Lone-Pair-Induced Anharmonic Rattling, Angew. Chem. Int. Ed. 55 (2016) 7792–7796. doi:10.1002/anie.201511737.